Surface plasmons in liquid mercury: Propagation in a nonuniform transition layer

Howard L. Lemberg*
Bell Laboratories, Murray Hill, New Jersey 07974
Stuart A. Rice and Daniel Guidotti
The Departments of Chemistry and Physics and The James Franck Institute, The University of Chicago, Chicago, Illinois 60637

(Received 22 April 1974)

We have examined the propagation of nonradiative surface plasmons in the presence of an inhomogeneous transition zone in the surface region of a conductor. The model we treat in the present paper is the Epstein stratified conductivity profile that has been proposed by Bloch and Rice for liquid mercury. Assuming that photon-plasmon coupling occurs through frustrated total reflection, we evaluate the optical response of mercury to surface-plasmon excitation and find it to be sensitive to the existence of such a zone. Measurements of the dispersion relation should, therefore, provide valuable information regarding the range and degree of such electronic inhomogeneity; preliminary measurements are in good agreement with the theory (Sec. VI). In addition to inhomogeneity in the conductivity of nearly-free electrons in the liquid metal, we have also investigated the effect of the localized resonances near the surface, and we speculate under what conditions the surface-plasmon dispersion relation may exhibit "anomalous dispersion" due to plasmon–localized-state interaction. Finally, the existence of an upper plasmon branch induced by the inhomogeneity is treated. In general, the results of the present investigation suggest that optical surface-plasmon spectroscopy should be a useful technique for the study of nonuniform conducting surfaces.

I. INTRODUCTION

Since the work of Bohm and Pines[1] the investigation of the properties of plasmons has been used to provide information regarding the electronic properties of metals and semiconductors. One of the most fruitful avenues of research in this regard has been the study of departures from idealized models of electronic behavior, such as the nearly-free-electron description of electronic conduction in metals,[2] or the simplified two-band picture which is used as a basis for understanding the optical properties of semiconductors.[3] Thus, the dispersion and damping of bulk plasmons, as determined by electron energy loss or optical methods, have been useful in probing a host of interactions between collective electronic oscillations and single particles or other collective modes in conducting media.[4–7]

Following a prediction by Ritchie,[8] there has in recent years been much interest in a second class of oscillations, surface-plasma waves,[9] which are observed at the surface of a bounded conducting medium (in addition to the bulk mode which exists in the interior). The most basic and one of the most frequently employed models for the surface mode involves the charge oscillations which occur at a plane boundary of zero thickness between a homogeneous free-electron metal and a homogeneous nonabsorbing dielectric. Surface plasmons in this geometry are associated with electric and magnetic fields of the form

$$\vec{F}(x, y, z, t) = \vec{F}_0 e^{i(k_x x - \omega t)} e^{\pm \kappa_i z} , \qquad (1.1)$$

where $\kappa_{m,d} = [k_x^2 - (\omega/c)^2 \epsilon_{m,d}]^{1/2}$ and ϵ_m, ϵ_d are the dielectric constants of the metal and dielectric, respectively. The waves propagate parallel to the interface (along the x direction) and are exponentially attenuated in the normal direction in both metal and dielectric.

Departures of the surface mode from the idealized behavior of (1.1) arise from a number of sources. Such deviations may, for example, represent electronic interactions of a sort similar to those in the bulk conductor. Thus, the effects of intraband damping[10] and phonon coupling[11] on plasmons may be understood qualitatively, though not quantitatively, in similar terms for the bulk and surface waves. Alternatively, departures of surface-plasma waves from model behavior may indicate the presence of surface structures on a microscopically large scale, as in the case of metal interfaces which have been intentionally roughened to permit photon-plasmon coupling.[12] Effects of this nature have also been used to investigate the presence of thin dielectric layers, such as metal oxides, on conducting surfaces.[13,14]

A third class of departures, which has thus far been only briefly considered as an influence on surface-plasma waves, may be ascribed to the fundamental distinction between a geometric boundary of zero thickness and the flat surface of a real metal, for which there must be electronic relaxation over several angstroms. In the surface region of a real metal interactions among the conduction electrons, and between electrons and metal ions, result in electronic transport properties and time-averaged charge distributions which are qualitatively different from those encountered in the bulk because of spatial variation in the dielectric

screening.[15] Thus, the surface region of a metal undergoes a well-known charge redistribution,[16] and in certain cases supports localized surface states also.[17]

It has recently been suggested by Bloch and Rice[18] that in the case of liquid mercury, a metal whose electronic properties are naturally quite structure-sensitive, the tendency towards electronic relaxation at the surface may be particularly pronounced. They propose a phenomenological model for the mercury surface which is based upon the notion that, in the liquid metal, the ion cores as well as the conduction electrons must exhibit a gradual decrease in density—not necessarily monotonic—from the bulk concentration to zero. Although far from rigorous, this view of the liquid-mercury surface incorporates a number of physical features which are expected on the basis of detailed microscopic treatments of metallic[19] and liquid[20] surfaces. On an experimental level, the postulated surface transition zone is consistent with available optical data,[18,21–23] which have been obtained by ellipsometric and near-normal reflection techniques.

We address ourselves in the present paper to the effects that a surface transition zone would have on the propagation of surface plasmons in mercury. Our interest in surface plasmons in liquid mercury has been motivated by several factors. First, the existence of collective electronic excitations such as surface plasmons in liquid metals has not been much investigated. To what extent such collective modes will persist in mercury, in spite of its rather low conductivity, seems a compelling question in its own right. Second, there has been a great deal of interest recently in the nature of surface plasmons at imperfect surfaces. In spite of the proposal of rather detailed models of photon-plasmon interactions in the presence of surface roughness,[24] though, there has been relatively little attention directed towards treatment of what is mathematically the simplest imperfect surface: a surface transition zone, within which the electronic properties are a continuous function of one spatial coordinate. Finally, the existence of a mode which is localized at an interface, as is the surface plasmon, immediately suggests the possibility of using that mode in surface diagnostic studies. The degree of sensitivity which the surface plasmon exhibits to the nonuniform surface zone of liquid mercury is thus a question of some significance, as it reflects both on the character of surface-plasma waves at inhomogeneous interfaces and on future studies of the surface properties of liquid metals. A preliminary report of the present work has appeared elsewhere.[25]

With the multiple objectives expressed above, we find it advantageous to review and develop the two topics separately in order to make the exposition of the work clear. Section II, therefore, summarizes the experimental evidence, which suggests the existence of anomalous surface structure in liquid mercury and mercury alloys. In particular, we describe the surface profiles which have been fit to experimentally observed optical constants. Section III outlines the local-dielectric-function theory of surface-plasma waves, with emphasis on those aspects which figure prominently in the subsequent discussion of surface plasmons at the anomalous mercury surface. A description of the numerical procedures and calculated results for the propagation of surface-plasma waves at an Epstein stratified mercury surface is provided in Sec. IV and the Appendix. Some care is taken in definition of the surface mode, for the strong damping of electronic motion in mercury makes the traditional approach, based on free-electron theory, not directly applicable. Radiative damping in optical excitation of the plasmon is discussed in detail. The conclusions of the present study, and some speculations about future studies of the spectrum of surface-plasma oscillations at nonuniform interfaces, are presented in Sec. V. Finally, at the request of the referee, we have included in Section VI a description of the results of preliminary measurements of the surface-plasmon dispersion relation for liquid Hg; agreement with theory is good.

II. SURFACE TRANSITION ZONE OF LIQUID MERCURY

A. Bloch-Rice model: Traditional optical investigations of mercury

After a period of controversy in the 1960's, the disputed optical constants of liquid mercury were reconciled by Bloch and Rice.[18] They proposed that the traditional methods of deducing the real and imaginary parts of the dielectric constant, ϵ_1 and ϵ_2, from experimental data had to be modified to take account of the inhomogeneous transition zone that exists at the surface of liquid mercury even under conditions of absolute purity. Within this zone, it was argued, the electronic properties could be significantly different from those of the bulk liquid metal because of inhomogeneities in both the electron and ion equilibrium densities, resulting in a nonuniform profile for the electric conductivity σ, which departed from the step-function behavior

$$\sigma(z) = \sigma\Theta(z) \tag{2.1}$$

assumed since the time of Drude.[26]

Employing a transition layer characterized by an Epstein profile[27] for the conductivity,

$$\sigma(w) = \frac{-w}{1-w}\left(\sigma_b + \frac{\sigma_s}{1-w}\right), \qquad w = -e^{2\pi z/\Delta}, \tag{2.2}$$

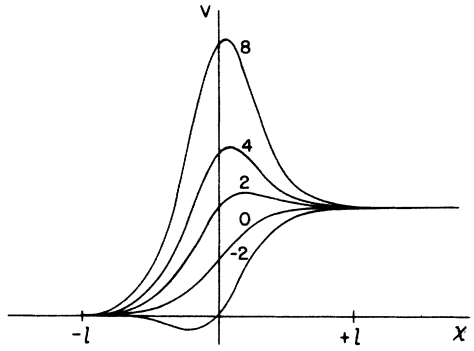

FIG. 1. Schematic of the Epstein profile, after Eckart (Ref. 27). The coordinate V, in Eckart's notation, corresponds to the conductivity σ; x and l represent the normal coordinate z and profile "half-width" Δ of the present work. The curves are parameterized by different values of σ_s/σ_b.

Bloch and Rice explained discrepancies between the apparent optical constants of mercury as determined by ellipsometric[21,22] and normal-incidence reflection techniques.[18] Because these experiments were performed at different angles of incidence, the apparent optical constants (the values of ϵ_1 and ϵ_2 that would characterize bulk mercury if the surface zone were of zero thickness) had been affected to different degrees by the presence of a surface layer of nonzero thickness. In equation (2.2) z is the coordinate normal to the liquid-metal surface; σ_b and σ_s represent frequency-dependent bulk and surface contributions to the conductivity. For positive values of the ratio σ_s/σ_b the profile starts from $\sigma \approx 0$ at $z \to -\infty$, increases and goes through a maximum near $z=0$, and then monotonically approaches the bulk value σ_b as $z \to +\infty$ (see Fig. 1).

To use (2.2) in the interpretation of optical data the dispersion relations for σ_b and σ_s must be known. Clearly, different dispersion relations will lead to different predictions. In the absence of complete information only simple models of σ_b and σ_s are worth pursuing. Thus, a subsidiary, but important, assumption of the Bloch-Rice model is that σ_b is described by a Drude frequency dependence

$$\sigma_b(\omega) = \frac{\sigma_{0b}}{1 - i\omega\tau_b} \ , \tag{2.3}$$

throughout the transition zone, with dc conductivity given by

$$\sigma_{0b} = ne^2\tau_b/m_e \ . \tag{2.4}$$

In (2.4) τ_b is the bulk relaxation time; e and m_e, the electronic charge and mass. It is assumed that each metal atom contributes both valence electrons to the pool of nearly-free electrons, whose concentration is n. For the surface contribution σ_s to the total conductivity, Bloch and Rice assumed a Drude form

$$\sigma_s(\omega) = \frac{\sigma_{0s}}{1 - i\omega\tau_s} \tag{2.5}$$

on the "bulk" side of the conductivity maximum, and a Lorentzian form

$$\sigma_s(\omega) = \frac{i\sigma_{0s}\omega\gamma}{(\omega_0^2 - \omega^2) - i\omega\gamma} \tag{2.6}$$

characteristic of localized-state conduction when the coefficient of the surface term, $-w/(1-w)^2$, falls below 70% of its maximum value. The shift in functional form for σ_s can be thought of as a Mott transition[28] which occurs as the mercury density drops from its bulk value to zero.

With expressions (2.3), (2.5), and (2.6) describing the various contributions to the conductivity, the Epstein profile (2.2) was fitted to the experimental results of Hodgson,[22] Faber and Smith,[21] Schultz,[23] and Bloch and Rice[18] in the energy range 0.6–3.0 eV. The parameter values producing the best fit were $\Delta = 6.28$ Å, $\sigma_{0s} = 48\sigma_{0b}$, $\tau_s = 0.9\tau_b$, $\gamma = \tau_s^{-1}$, and $\hbar\omega_0 = 0.6$ eV. The somewhat unphysical nature of these values was judged as an indication of incompleteness, rather than fundamental inaccuracy, of the model.

A second and comparable fit to the experimental data was found by permitting the decay length of the Epstein profile to become different in the surface regions of quasifree and localized electronic states. Physically, one recognizes that relaxation of the charge distribution at the liquid-metal surface is a function of the effectiveness of electronic screening, which certainly must differ for the two types of states. The final parameter values for the skewed profile were $\Delta_1 = 6.28$ Å, $\Delta_2 = 31.42$ Å, $\sigma_{0s} = 17\sigma_{0b}$, $\tau_s = 0.9\tau_b$, $\gamma = \tau_s^{-1}$, and $\hbar\omega_0 = 0.8$ eV, with localized states occurring in the region of smaller decay length.

Experimental work on the optical properties of liquid metals has proceeded in several directions since the investigations of Bloch and Rice. In a series of thorough ellipsometric and reflectance measurements, Crozier and Murphy[29] have verified the influence of the postulated transition zone on the optical properties of mercury. They perform both experiments on the same samples, finding differences between the apparent optical constants which are comparable to those noted by Bloch and Rice. The possibility that these discrepancies could have been due to surface contamination in a number of previous determinations—already remote because of relative internal consistency of the two sets of experimental values for ϵ_1 and ϵ_2—is thereby eliminated. Crozier and Murphy fit their observations to an Epstein profile

with the same parameters as Bloch and Rice, but with one additional ingredient: a cutoff on the low-density vapor tail, resulting in elimination of part of the localized-state region, when mercury is bounded by a dielectric window instead of a vacuum. This feature increases the plausibility of the proposed surface zone without changing its basic character. The vectorial nature of the optical properties is also emphasized by these authors: The effective values of ϵ_1 and ϵ_2 for p- and s-polarized light differ in the presence of a surface transition layer because the electronic response of the medium deviates from that of a homogeneous, isotropic metal. Thus, in reflectance studies performed far from normal incidence, the properties of the surface layer are weighted to an extent that depends on the incident polarization.

Among the other investigations of liquid mercury which have in recent years provided support for the reality of a surface transition layer, the work of Comins[30] and Choyke, Vosko, and O'Keeffe[31] should also be mentioned. The ellipsometric measurements of Comins, performed in the infrared, corroborate the character of the Hodgson "bend" in the dependence of ϵ_1 on wavelength, separating spectral regions of monotonically increasing and decreasing ϵ_1. To date this behavior has been successfully explained only by the surface-zone model. At higher energies ($\approx 1-8$ eV) Choyke, Vosko, and O'Keeffe have measured the dielectric functions of liquid and solid mercury with ellipsometic and normal-incidence methods, finding (by traditional interpretation) two sets of optical constants which show significant differences for the liquid phase. The ellipsometric values are approximately 10–20% greater in absolute magnitude than the values deduced from reflectance.

Investigations of a somewhat different type have been conducted by Siskind, Boiani, and Rice,[32] whose extensive near-normal-incidence reflectance measurements on liquid mercury-indium alloys have been aimed at elucidating the bulk electronic properties of such systems as well as the effect of alloying on the inherent transition layer of mercury.

In the low-energy region ($\hbar\omega \leq 8$ eV), these workers find it necessary to incorporate the effect of a surface transition zone in order to understand the non-Drude behavior of the apparent optical constants of the amalgams. In addition to the physical transition zone which occurs in mercury, differing concentration profiles for the two types of ion core may now appear, this new feature reflecting the tendency of a component of low surface energy (in this case, mercury) to preferentially populate the superficial region of a mixture.[33] Mathematically this effect is provided for by assuming that σ_b in (2.2) can depend on z, as well as ω, in the following fashion:

$$\sigma_b(\omega, z) = \sigma_b(\omega, 0), \quad z < 0$$

$$\sigma_b(\omega, z) = \sigma_b^*(\omega) + [\sigma_b(\omega, 0) - \sigma_b^*(\omega)]\, e^{-z/\Lambda}, \quad z \geq 0 \tag{2.7}$$

where $\sigma_b^*(\omega)$ is the bulk alloy conductivity and Λ a decay length which measures the variation of $\sigma_b(\omega, z)$ from its surface value of $\sigma_b(\omega, 0)$ to the bulk value. Typically, $\Lambda = 30$ Å and the parameter values of the skewed Epstein profile cited above achieve reasonable fits to the optical constants of the mercury-indium alloys.

B. Improving on conventional optical techniques: Criteria for a more sensitive probe

The experimental work of Bloch and Rice on mercury, as well as the subsequent investigations described above, have thus far been based upon the techniques of conventional reflection spectroscopy: At a fixed angle of incidence, either the reflected intensity is studied as a function of incident frequency, as in near-normal reflectance, or the phase change and absolute value of the ratio of reflected amplitudes is measured, as in ellipsometry. Then, if it is assumed that the material under study is homogeneous and that all boundaries are of zero thickness, optical constants can be deduced from either set of measurements, in conjunction with a Kramers-Kronig inversion in the case of reflectance[34] and the classical Fresnel relations[35] in the case of the ellipsometric data.

When the surface properties of a material differ significantly from those of the bulk, however, the procedure for determining optical constants from experiment is not at all straightforward. There are fundamental ambiguities in the interpretation of such results to yield information regarding either surface or bulk structure, unless the two give rise to distinct absorptive mechanisms. Molecules adsorbed on metal surfaces provide an example of the latter behavior, frequently producing infrared absorptions that are well correlated with vibrational bands of the parent molecule.[36] But when the anomalous surface structure is an inherent feature of the material being considered, one is often limited to fitting simple or plausible models of surface structure to observations and relying on similarly reasonable models of the bulk. In the case of a transition zone one is faced with a special difficulty: By means of the Herpin matrices[37] it may be shown that any region of continuous, nonuniform structure is equivalent optically to a discrete system consisting of only two homogeneous layers. The broad implication of this equivalence is that optical measurements of quantities such as reflectivities or phase changes upon reflection are nonuniquely related to the struc-

ture of the inhomogeneous region.

For the reasons expressed above, conventional optical techniques are subject to important limitations in their sensitivity to the presence of a nonuniform transition zone whose width is much smaller than the wavelength of the incident light. This consideration, coupled with the desire to gain a better understanding of the electronic structure of the liquid metal surface, has motivated us to ask what new types of experimental investigations should be responsive to surface structure, particularly the type proposed for mercury. In the present inquiry attention has been limited to probes which utilize electromagnetic radiation, as these are among the simplest and most direct. More sophisticated methods, such as low-energy-electron diffraction (LEED), are in principle more sensitive to surface properties, since the scattering events which determine LEED profiles take place in the first few atomic layers.[38] But at the present time the energy and angular resolution of such experiments, and the existence of serious uncertainties in their theoretical interpretation, combine to reduce the accuracy and value of the information which can be obtained.[39,40]

Restricting the scope of possible experiments, then, we note that one of the qualitative factors influencing our choice is the existence of a classical penetration depth of electromagnetic radiation into a conductor,[41]

$$\delta = c/(2\pi\omega\sigma_0)^{1/2} . \tag{2.8}$$

For metallic conductors the penetration depth is essentially independent of the angle of incidence of the radiation, for the derivation of (2.8) is based on the assumption that $\mathrm{Re}(4\pi\sigma/\omega) \gg 1$. In ellipsometric and normal-incidence studies of liquid mercury, therefore, attenuation of the incident beam in the direction normal to the metal surface is described by a common decay length, Eq. (2.8).

The observation of a common penetration depth prompts us to inquire why ellipsometric investigations of mercury seem more sensitive to the existence of a surface zone. It has been argued[29] that this enhanced sensitivity arises because ellipsometric experiments sample the response of the metal to incident electric fields that are both normal and parallel to the interface, while at near-normal incidence most of the incident field strength is in the parallel direction. If we consider the boundary conditions across a metallic interface we find support for this viewpoint, for the requirement of continuity of the tangential electric field across the interface implies that the normal field must vary much more rapidly in the surface region—even near a sharp zero-thickness interface. Hence any deviation away from zero thickness, such as the existence of a transition zone, should exert a more pronounced influence on the reflection of p-polarized radiation than it does for s polarization.

The preceding discussion suggests that the class of experiments which should permit the study of the transition zone of a liquid metal with reasonable sensitivity is that which allows for a small penetration depth, and which also employs an incident field that induces a large electronic response in the normal direction. One means of satisfying these conditions is by selection of a probe which obeys a different dispersion relation from those associated with the standard optical method and which makes maximum use of p-polarized radiation. The nonradiative surface plasmon (NRSP)[9] is just such a probe. The NRSP couples exclusively to p-polarized light and has a dispersion curve which lies primarily to the right of the light line of the adjacent contact medium, in contrast to the radiative dispersion relations which define other optical properties (see Fig. 2). Moreover, as an electronic excitation which is intrinsically localized to the surface region of a conductor, the NRSP should manifest some degree of sensitivity to the gross electronic structure of a surface zone such as that described by (2.2). To amplify a bit, it has already been pointed out that for ellipsometry or normal-incidence reflectance, the angle of incidence θ is usually a fixed parameter. The relation between frequency and wave vector of the incident and reflected light is consequently linear,

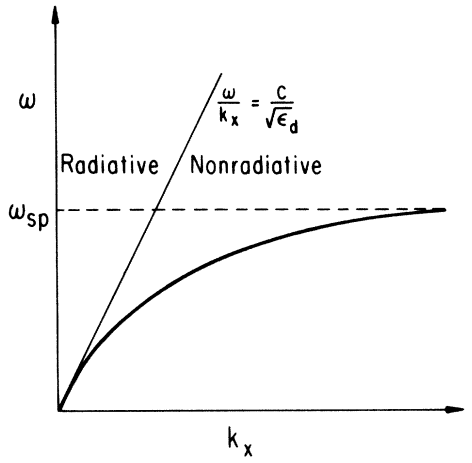

FIG. 2. Approximate form of the nonradiative surface-plasmon dispersion, at a free-electron-metal–dielectric boundary of zero thickness. The phase velocity of light in the dielectric is $c\epsilon_d^{-1/2}$, $\epsilon_d^{1/2}$ being the index of refraction. Waves of greater phase velocity lie in the radiative regime, and are able to couple directly to light; excitations with smaller phase velocities are nonradiative. For a metal characterized by free-electron conduction near the plasma frequency, the frequency of the surface plasmon ω_{sp} is just $\omega_p(1+\epsilon_d)^{-1/2}$.

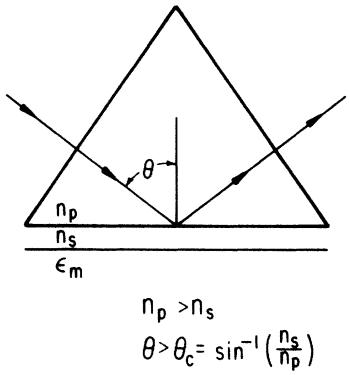

FIG. 3. Experimental configuration for the method of frustrated total reflection. A prism of high refractive index (n_p), undercoated with a low-index (n_s) dielectric spacing film, is bounded by a semi-infinite metal with dielectric function ϵ_m. For angles of incidence greater than the critical angle for total reflection, θ_c, light may be absorbed by the NRSP which propagate along the s-m interface.

with

$$k_x = (\epsilon_d^{1/2}\omega/c)\sin\theta \ . \qquad (2.9)$$

Equation (2.9) may be considered the dispersion relation which characterizes these standard methods of optical experimentation. Such investigations are obviously confined to the radiative range $k_x \leq \epsilon_d^{1/2}\omega/c$ for real angles of incidence. Now, Eq. (2.8) holds for real angles of incidence and good conductors. More generally, the penetration of radiation normal to the conducting surface is governed by the quantity $\kappa_m = [k_x^2 - (\omega/c)^2\epsilon_m]^{1/2}$, the exact skin depth δ being given by

$$\delta = \frac{1}{\mathrm{Re}(\kappa_m)} = \frac{c}{\omega}\,\frac{1}{\mathrm{Re}[(\epsilon_d \sin^2\theta - \epsilon_m)^{1/2}]} \ . \qquad (2.10)$$

Since liquid mercury is a relatively poor conductor of electricity, the unapproximated form (2.10) is retained here to illustrate the dependence of δ on both the (possibly complex) angle of incidence and on the sizable imaginary part of ϵ_m in mercury.

In contrast to the linear "dispersion" of common optical methods, note from Fig. 2 that the NRSP dispersion curve, although approximately linear in the low-energy range, becomes extremely nonlinear as energy increases. This nonlinearity, which distinguishes surface-plasmon absorption from ellipsometry and reflectance, has important physical consequences for the response of the conducting surface to nonradiative surface-plasma waves. In the frequency range between $\omega \ll \omega_{sp}$ and $\omega \approx \omega_{sp}$, the wave vector of the excitation varies from $k_x \approx \epsilon_d^{1/2}\omega/c$ to $k_x \gg \epsilon_d^{1/2}\omega/c$. It is readily seen from (2.10), then, that the skin depth for surface-plasmon absorption will in general be somewhat smaller than corresponding values of δ for ellipsometric or normal-incidence experiments performed at the same energy. Hence, in the intermediate- and high-energy regions, where deviation of the NRSP dispersion curve from the dielectric light line is expected to be large, the NRSP should be more sensitive to the over-all structure of the surface zone than other experimental methods based on simple reflection spectroscopy.

The most convenient method by means of which one can couple incident electromagnetic radiation to the NRSP is frustrated total reflection (FTR), a technique first clearly articulated and exploited for this purpose by Otto.[42] In recent years FTR has been widely used in the study of surface excitations of many types.[43–45]

The FTR configuration, illustrated in Fig. 3, enables one to sample that portion of the frequency–wave-vector plane between the light line of the prism, $\omega = ck_x/n_p$, and that of the dielectric spacing layer, $\omega = ck_x/n_s$, by varying θ, the angle of incidence on the prism base, and the frequency ω. By utilizing the total reflection properties of the prism-film coupler, one can generate evanescent light waves of the same phase velocity as the NRSP, and it thereby becomes possible to conserve both energy and momentum in exciting the surface plasmon. The resonance condition is clearly indicated in Fig. 4. Relatively efficient coupling between incident light and the nonradiative mode can be accomplished in this manner.

The dispersion relation for surface plasmons excited through the prism-film coupler is actually somewhat different from the simple form charac-

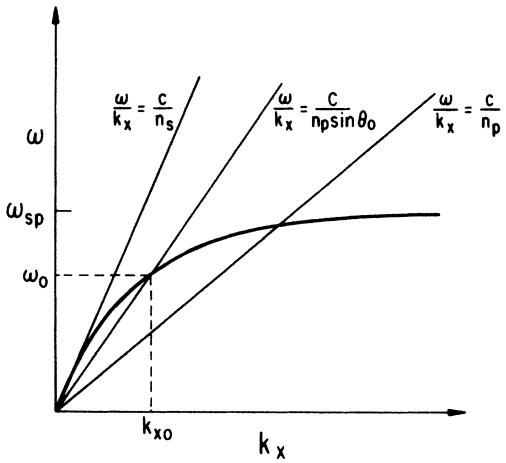

FIG. 4. Coupling to nonradiative excitations by frustrated total reflection. At a particular angle of incidence, $\theta_0 > \theta_c$, on the prism base (see Fig. 3), light can satisfy the resonance conditions for NRSP excitation, with resonant frequency and wave vector given by ω_0 and k_{x0}, respectively.

teristic of a metal–single-dielectric interface, since introducing the thin dielectric layer changes the character of the boundary-value problem that must be solved. Within the film there are evanescent waves decaying in $+z$ and $-z$ directions, one resulting from the response of the polarization to surface-plasma waves at the s-m interface, the other associated with total reflection at the p-s interface. In a simple ray-optics picture, the two decaying waves undergo multiple reflection at the two interfaces, and a self-consistent field is established in the dielectric which differs from the field that would exist in a semi-infinite dielectric. The requirement of self-consistency, contained implicitly in the boundary conditions which are employed, introduces a small quantitative change in the character of the surface-plasmon dispersion relation in addition to allowing optical coupling to occur in the first place.

III. LOCAL-DIELECTRIC-FUNCTION DESCRIPTION OF SURFACE PLASMONS

The microscopic basis of the theory of surface plasmons has been a subject of sophisticated theoretical development[46,47] and elaborate model-based calculations[48,49] in recent years. In the optical regime which interests us, however, it is sufficient to consider the NRSP in a local-dielectric-function framework of the type employed by Bloch and Rice for the analysis of classical reflectivity and ellipsometry measurements.

The simplest approach to the theory of surface-plasma waves is based on the form that Maxwell's equations[50] assume in a conducting medium:

$$\nabla \cdot \vec{\mathfrak{D}} = 0 , \tag{3.1a}$$

$$\nabla \cdot \vec{\mathfrak{B}} = 0 , \tag{3.1b}$$

$$\nabla \times \vec{\mathcal{E}} = -\frac{\mu}{c}\frac{\partial \vec{\mathcal{H}}}{\partial t} , \tag{3.1c}$$

$$\nabla \times \vec{\mathcal{H}} = \frac{1}{c}\frac{\partial \vec{\mathfrak{D}}}{\partial t} + \frac{4\pi}{c}\vec{\mathcal{J}} , \tag{3.1d}$$

where $\vec{\mathfrak{D}} = \epsilon_c \vec{\mathcal{E}}$, $\vec{\mathfrak{B}} = \mu \vec{\mathcal{H}}$, and c, of course, is the velocity of light. The conduction current density $\vec{\mathcal{J}}$ is given by Ohm's law,

$$\vec{\mathcal{J}} = \sigma \vec{\mathcal{E}} , \tag{3.2}$$

which should be valid except under conditions where the anomalous skin effect becomes important.[51] For the range of energies considered in the present investigation corrections to (3.2) should not be significant. It may be assumed, in addition, that the magnetic permeability μ and the real dielectric constant ϵ_c (which arises from internal polarization of the ion cores)[52] are both unity.

Equation (3.1a) is a nontrivial statement about the nature of surface-plasma waves, for it expresses the fact that no longitudinal charge oscillations are associated with the surface mode, in contrast to the fundamental character of plasma waves in the bulk.[53] For the relatively low frequencies $\omega < \omega_{sp}$ (the surface-plasmon frequency) at which the NRSP is observed it is well known that a conducting medium cannot sustain local charge fluctuations. Departures from (3.1a) may become important, however, for the higher-frequency, $\omega \gtrsim \omega_{sp}$, radiative surface modes which have been mentioned in the literature.[9]

The electric and magnetic fields are now assumed to depend on time in a simple harmonic fashion,

$$\begin{aligned} \vec{\mathcal{E}}(x,y,z,t) &= \vec{\mathrm{E}}(x,y,z)\, e^{-i\omega t} , \\ \vec{\mathcal{H}}(x,y,z,t) &= \vec{\mathrm{H}}(x,y,z)\, e^{-i\omega t} , \end{aligned} \tag{3.3}$$

in which case the two curl equations (3.1c) and (3.1d) take the form

$$\nabla \times \vec{\mathrm{E}}(x,y,z) = (i\omega/c)\, \vec{\mathrm{H}}(x,y,z) , \tag{3.4a}$$

$$\nabla \times \vec{\mathrm{H}}(x,y,z) = -(i\omega/c)(1 + 4\pi i\sigma/\omega)\, \vec{\mathrm{E}}(x,y,z) . \tag{3.4b}$$

We now define the complex dielectric constant of the metal as

$$\epsilon = 1 + 4\pi i\sigma/\omega , \tag{3.5}$$

which has the effect of incorporating the conduction current implicitly into the displacement current. With (3.5), (3.4b) reduces to

$$\nabla \times \vec{\mathrm{H}}(x,y,z) = -(i\omega\epsilon/c)\, \vec{\mathrm{E}}(x,y,z) . \tag{3.6}$$

Equations (3.1a), (3.1b), (3.4a), and (3.6) express Maxwell's equations in the form most convenient for the present analysis, as they may be applied to either dielectric or metallic media simply by substituting the appropriate dielectric constant ϵ_i of medium i. These dielectric constants may, in general, depend on the frequency ω, and in the liquid metals which are discussed here, we allow for possible coordinate dependence of ϵ_i because of the existence of a surface transition zone. In the long-wavelength limit which the present work treats, we assume that all of the ϵ_i are independent of wave vector $\vec{k}$. This assumption is physically consistent with the local relation (3.2) between the current density and the electric field.

Surface plasmons are known to interact with only p-polarized radiation. Taking the plane of incidence to the xz plane, then, we set $E_y \equiv 0$ and assume that all fields are independent of the coordinate y; $H_x \equiv 0$ and $H_z \equiv 0$ follow directly. The geometry is specified by supposing the half-space $z \geq 0$ to be occupied by liquid metal, and the region $z < 0$ by a semi-infinite dielectric. Finally, we may assume, without loss of generality, that all fields display x dependence of the form $e^{ik_x x}$. With these

simplifications, the field equations reduce to the form characteristic of transverse-magnetic (TM) waves:

$$\frac{\partial E_x}{\partial z} = ik_x E_z + \frac{i\omega}{c} H_y , \tag{3.7a}$$

$$\frac{\partial H_y}{\partial z} = \frac{i\omega\epsilon}{c} E_x , \tag{3.7b}$$

$$E_z = -\frac{ck_x}{\omega\epsilon} H_y . \tag{3.7c}$$

After some straightforward algebra, Eqs. (3.7) yield a second-order differential equation for the tangential magnetic field,

$$\frac{\partial}{\partial z}\left(\frac{1}{\epsilon}\frac{\partial H_y}{\partial z}\right) = \frac{\kappa^2}{\epsilon} H_y , \tag{3.8}$$

with $\kappa^2 = k_x^2 - (\omega/c)^2\epsilon$. For the case that the (semi-infinite) metal is homogeneous up to a geometrically plane surface which is the boundary between it and a semi-infinite dielectric, Eq. (3.8) is readily solved. One then obtains, easily, the dispersion relation of the surface plasmons. For the case considered herein, namely, an inhomogeneous boundary between bulk metal and dielectric, Eq. (3.8) is difficult to solve; this will be discussed in the Sec. IV.

The damping of surface plasmons can be described in the local theory by taking the dielectric function to be complex. In general, when the dielectric function $\epsilon_m(\omega)$ has a nonzero imaginary part the resonant NRSP wave vector k_x must become complex also. Two interpretations can be attached to the complex character of k_x: On the one hand, since the propagation of surface-plasma waves along the conductor-dielectric interface is described by the exponential factor $e^{ik_x x}$, the quantity $\mathrm{Im}k_x$ may be regarded as the inverse of a mean free path for the NRSP. This point of view has been adopted recently by Bell *et al.*[54] in a study of coupled plasmon-phonon modes in the semiconductor InSb. On the other hand, one may equivalently consider the imaginary part of k_x as a measure of the angular half-width of the surface-plasmon absorption at some fixed, real value of the frequency. This alternative interpretation has been expressed by Otto[42] in the relation

$$\mathrm{Im}k_x = (\epsilon_d^{1/2}\omega/c)\cos\theta(\omega)\,\Delta\theta(\omega) , \tag{3.9}$$

where $\theta(\omega)$ is the resonant angle of incidence determined by the "real" dispersion relation between ω and $\mathrm{Re}k_x$.

IV. CALCULATIONS AND RESULTS FOR THE LIQUID-METAL TRANSITION ZONE

The study of nonradiative surface plasmons in liquid mercury by solution of Eq. (3.8), with inclusion of the effect of a nonuniform transition zone, is hindered from the outset by the fact that the analytic structure of the Epstein profile does not permit exact solution of (3.8) in terms of known functions. This limitation has made it impossible in the present work to obtain a dispersion relation in closed form for the mode which is strictly bound to a diffuse mercury-dielectric interface. For the sake of completeness, nevertheless, we sketch here the course which a method based on numerical integration might take in evaluating the dispersion and damping of such a bound surface-plasma mode.

We assume a semi-infinite dielectric d filling the half-space $z<0$; the liquid metal, with its transition zone, occupies the region $z \geq 0$. Although the surface layer is characterized by continuous spatial variation of its properties, one can identify, with some degree of arbitrariness, a fictitious surface at some $z=h$ which "separates" bulk mercury from the transition region. At this position the dielectric constant $\epsilon_m(z)$ has nearly decayed to its asymptotic bulk value, ϵ_b. The tangential magnetic field, from which we can determine the dispersion and damping of the surface mode, is now given by

$$H_y = \begin{cases} A_d e^{\kappa_d z}, & z<0 \\ H_y(z), & 0 \leq z \leq h \\ B_m e^{-\kappa_m z}, & h<z \end{cases} \tag{4.1}$$

in the three regions of space.

In order to integrate $H_y(z)$ numerically across the transition zone, it is necessary first to have a set of initial conditions. Such conditions are conveniently obtained by imposing a "normalization" requirement on one of the coefficients in (4.1). We choose to define B_m such that $B_m e^{-\kappa_m h} = 1$ and we then apply continuity conditions at $z=h$ to find that

$$H_y(h) = 1 , \tag{4.2a}$$

$$H_y'(h) = -\kappa_m . \tag{4.2b}$$

The normalization of B_m has no effect on the actual dispersion relation, as all the fields in (4.1) are arbitrary to within a common multiplicative constant.

Using the initial conditions (4.2), one can integrate across the transition zone from $z=h$ to $z=0$, where the surface layer is bounded by dielectric d. Boundary conditions at this second interface imply that

$$H_y(0) = A_d \tag{4.3a}$$

and

$$H_y'(0) = \kappa_d A_d/\epsilon_d , \tag{4.3b}$$

and, upon combining (4.3a) and (4.3b), we obtain the dispersion relation for surface plasmons in the presence of a surface transition layer:

$$\kappa_d/\epsilon_d - H_y'(0)/H_y(0) = 0 \ . \qquad (4.4)$$

Though not shown explicitly, the logarithmic derivative of H_y depends on the frequency and wave vector through conditions (4.2).

While the derivation of (4.4) is useful in illustrating the general features of a local theory of surface-plasma waves in liquid mercury, we observe, first of all, that the bound resonances implied by this dispersion relation are not really observed in optical experiments on metal surfaces since there is an incoming traveling wave in such experiments. For the specific case of liquid mercury, it should further be noted that the shift in character of the surface conductivity at a definite value of z makes direct numerical integration somewhat difficult, and would certainly complicate the sort of iterative scheme (in ω and k_x) which would be necessary to solve (4.4) with some degree of precision. For these reasons it is simpler to study surface plasmons in liquid mercury by considering directly the optical response of a diffuse mercury interface to excitation of surface-plasma waves by light.

In numerically evaluating the character of surface-plasma waves at the nonuniform mercury surface, we have utilized frustrated total reflection as the means of coupling light waves to the surface excitation. In principle, the prism-film coupler should disturb the fundamental nature of the surface transition zone least among the available techniques of optical coupling. Other methods of coupling to the liquid-metal surface plasmon should be possible, nevertheless: creation of a hydrodynamic grating by excitation of short-wavelength capillary waves is one such alternative. Rough surfaces have historically played a prominent role in the study of surface plasmons,[54,55] for the two-dimensional translational symmetry which is broken by the existence of roughness provides a source of quasimomentum parallel to the interface, allowing one to circumvent the problems of energy and momentum conservation in optical coupling to the NRSP.

The surface-plasmon dispersion which is reported in this section has been determined by numerically solving the field equation (3.8) for the waves which propagate (or decay) in the skewed Epstein stratified transition layer defined by Bloch and Rice. A method based on the Herpin matrices[37] has been employed in evaluating the optical response of mercury to NRSP excitation. As in standard treatments of the electrodynamics of stratified media, this algorithm approximates the full inhomogeneous profile by a pile of thin slices, each assumed to be homogeneous. Mathematical details of the procedure are described in the Appendix. The present application included a layer s, corresponding to the spacer film of the coupler, in addition to the thin slices of the inhomogeneous profile. Appropriate boundary conditions at the prism-film and metal-film interfaces were also employed. The refractive index of the prism was taken as $n_p = 2.53$ and that of the spacer as $n_s = 1.39$, typical values for available high- and low-index materials (such as KRS-5 and LiF) in the visible spectrum. They were assumed to be independent of frequency throughout the infrared, visible, and ultraviolet in order to simplify the computations. The spacer thickness d, a critical parameter in determining the extent of photon–surface-plasmon coupling and the degree of radiative damping of the excitation, depended on the frequency in a manner which will be described in detail below.

Typical results for the reflectivity of TM waves from mercury, calculated at fixed frequency and as a function of angle of incidence (on the prism base), are illustrated in Figs. 5–8. The figures demonstrate that surface-plasmon absorption at a diffuse interface should be measurably different from that at a perfectly sharp (zero-thickness) boundary with the effective optical constants measured by ellipsometry or reflectivity. The ellipsometric curves shown are based upon the measurements of Faber and Smith,[21] which extended to a maximum energy of about 3 eV. The plasmon is obviously photonlike at lower energies, its dispersion approaching the light line $\omega = ck_x/n_s$ as $\omega \to 0$. Even at these low energies (≈ 1–2 eV), though, there is a significant difference between the "per-

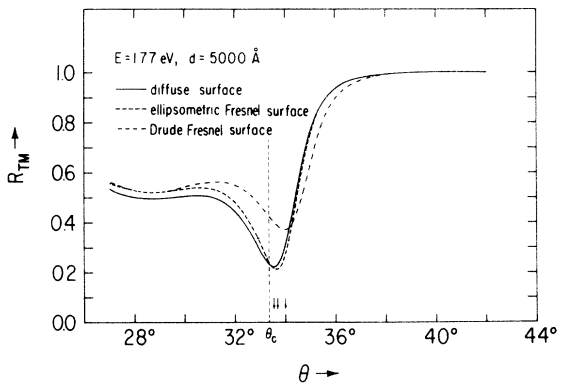

FIG. 5. Transverse-magnetic reflectivity R_{TM}, for $E = 1.77$ eV and three models of the liquid-mercury surface: diffuse, with skewed Epstein profile; sharp surface, with ellipsometric optical constants; sharp surface, with Drude optical constants. All computations performed for FTR geometry with spacer thickness d and parameter values described in the text. Arrows locate the abscissae of minimum reflectivity, or maximum coupling to the NRSP.

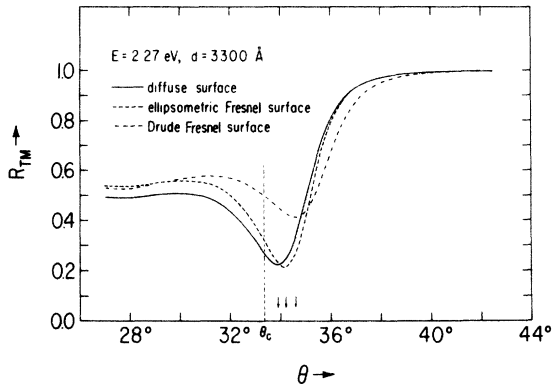

FIG. 6. Transverse-magnetic reflectivity R_{TM} for E = 2.27 eV and three models of the liquid-mercury surface. Computations as in Fig. 5.

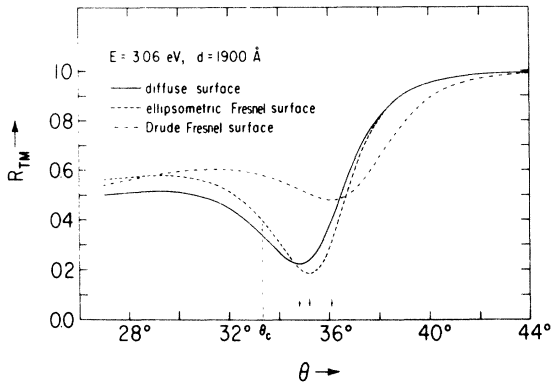

FIG. 8. Transverse-magnetic reflectivity R_{TM} for E = 3.06 eV and three models of the liquid-mercury surface. Computations as in Fig. 5.

fect-surface" Drude and the nonzero-thickness-transition-zone reflectivity minima. The ellipsometric sharp surface, although displaying behavior that is closer to calculations for a diffuse-surface model, should still be distinguishable from the latter by careful experimentation. This closer agreement is to be expected, of course, since the ellipsometric optical constants reflect a nonzero contribution from p-polarized light.

It is apparent from the figures that as the energy increases, the three surface models give rise to NRSP absorption which becomes increasingly different. Thus, at 1.77 eV, the angular separation of the reflectivity drops for diffuse and ellipsometric surfaces is only 0.1°; by 3.06 eV, it has increased to approximately 0.2°. The diffuse-surface and Drude minima, by way of comparison, are separated by 0.5° at 1.77 eV and 1.1° at 3.06 eV.

In order to evaluate "ellipsometric" Fresnel surface reflectivities at still higher energies

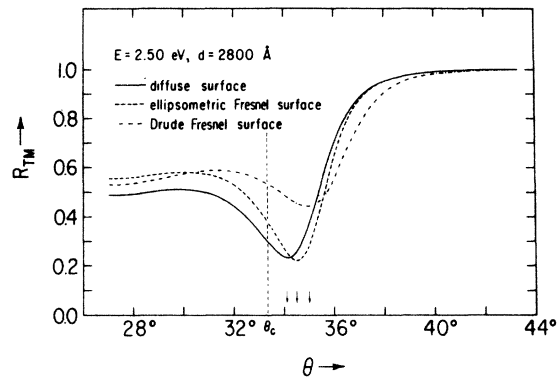

FIG. 7. Transverse-magnetic reflectivity R_{TM} for E = 2.50 eV and three models of the liquid-mercury surface. Computations as in Fig. 5.

(> 3.06 eV), where the differences between models are expected to be even more pronounced, it was necessary first to compute a set of apparent optical constants characterizing the mercury surface. These calculations were performed by evaluating r_p and r_s, the amplitude reflection coefficients for a vacuum–nonuniform-mercury interface, at 78° incidence, and then inverting the sharp-surface Fresnel relations to give apparent values for the real and imaginary parts of the dielectric constant ϵ_m. It is worth reemphasizing the significance of these constants for the subsequent analysis: They are the values of $\mathrm{Re}\epsilon_m$ and $\mathrm{Im}\epsilon_m$ that would be measured in an ellipsometric experiment *if the skewed profile were completely accurate*.

By employing this expedient, the apparent optical constants were evaluated for energies between 3 and 5 eV. The response of mercury to NRSP excitation is illustrated in Figs. 9–11 at these higher energies for the full profile, a Drude Fresnel surface, and an equivalent "ellipsometric" Fresnel surface. Once again the absorption should be measurably different for the three cases. The displacement between the lower two curves in this set of figures illustrates convincingly that the shifts observed in Figs. 5–8 are due to the inherent structure of the transition region, and are not simply an artifact of the slight deviation in the Bloch-Rice fit to ellipsometric measurements.

The NRSP dispersion relation may be determined over a range of energies by measuring the angle of minimum reflectivity, corresponding to maximum coupling to the excitation, from several sets of calculations. The effect of the surface zone, most noticeable at high energies, has been evaluated from 3.5 to 5.5 eV, where interband effects start to become important,[56] and is shown in Fig. 12. We note, in particular, the shift of the

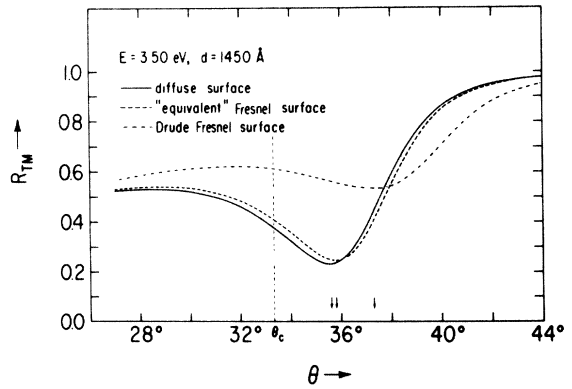

FIG. 9. High-energy reflectivity calculations, for $E = 3.50$ eV and three models of the liquid-mercury surface: diffuse, with skewed Epstein profile; sharp surface, with "equivalent" optical constants; sharp surface, with Drude optical constants. FTR parameters as in Fig. 5.

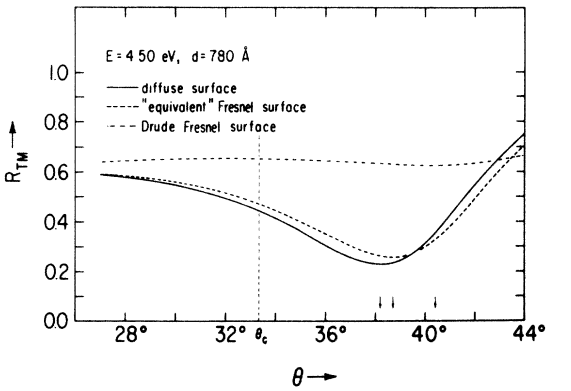

FIG. 11. High-energy reflectivity calculations, for $E = 4.50$ eV and three models of the liquid-mercury surface. Computations as in Fig. 9.

dispersion relation towards the radiative regime. This finding is consistent with the higher effective electron density in the transition region, and also agrees with a simpler metal-film–metal-substrate model in which the film plasma frequency is somewhat greater than that of the substrate.[57]

The curves shown in Fig. 12 correspond to the real part of the dispersion relation relating ω to $\mathrm{Re}k_x$. In addition to the positions of the minima in R_{TM}, the widths of the reflectivity drops in Figs. 5–8 and 9–11 are of interest, for these are a measure of the internal electronic damping in the liquid metal. Since mercury is a relatively poor conductor, with a short electronic relaxation time, the approximation $|\mathrm{Re}\epsilon_m| \gg |\mathrm{Im}\epsilon_m|$ is not valid; consequently, the peak width $\Delta\theta(\omega)$ is no longer related to $\mathrm{Im}\epsilon_m$ linearly as it is in (3.9). At low frequencies ($\hbar\omega \approx 1$ eV), in fact, the imaginary part of ϵ_m can be as large or larger than the real part, implying that the surface plasmon will be quite heavily damped in mercury relative to other metals. This is manifested in the large angular half-widths exhibited by the optical-response calculations. From Figs. 5–11 we note that the diffuse-surface and ellipsometric-Fresnel-surface models show absorptive half-widths which are approximately equal, the half-widths for the nonuniform surface being slightly larger. The Drude Fresnel-surface calculations, by contrast, show poorer over-all coupling to the surface plasmon and distinctly larger half-widths. As the energy increases we note a general trend toward increasing half-widths for all three surface models. This increase appears to be a limiting factor in our ability to define a surface-plasma mode at energies much above 5 eV.

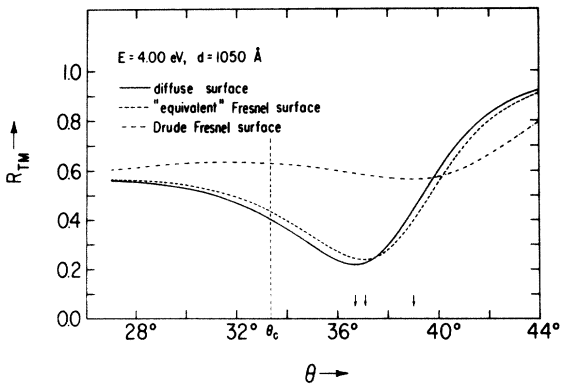

FIG. 10. High-energy reflectivity calculations, for $E = 4.00$ eV and three models of the liquid-mercury surface. Computations as in Fig. 9.

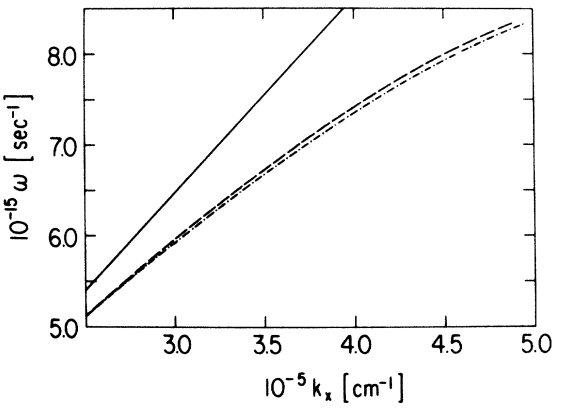

FIG. 12. Dispersion relation for surface plasmons at a liquid-mercury–dielectric interface, for FTR geometry. Dashed curve is dispersion relation for full inhomogeneous profile; dot-dashed line, for an ellipsometrically equivalent sharp surface. Absorption at a Drude sharp surface is heavily damped at these energies, so the resulting dispersion is not shown. Solid curve represents the light line $\omega = ck_x/n_s$ in the dielectric spacer layer.

In the determination of NRSP dispersion presented above for the mercury surface with a nonuniform conductivity profile, there are a number of points which deserve further elaboration. To simplify matters, we first discuss these questions for the surface plasmons at a hypothetical metal boundary of zero thickness. At a homogeneous metal surface, the NRSP has been identified as that mode of electronic oscillation which is completely bound to the metal-dielectric boundary. This defining condition must be generalized somewhat in the FTR geometry of Fig. 3; with two boundaries in close proximity, no mode exists which is strictly bound to the metal–thin-film interface. The surface plasmon is in this case specified by assuming there are only incoming light waves in the prism. As a result, the normal modes of charge oscillation correspond to complete frustration of the total reflection that is ordinarily anticipated for $\theta > \theta_c$.

Experimentally, however, the surface plasmon is rarely observed with complete absorption of incident radiation. One usually observes a distinct reflectance drop as a function of angle of incidence for fixed frequency (or vice versa), with the minimum of R_{TM} located in the neighborhood of the resonance angle (frequency). The magnitude of such a dip may range from as little as 10% to more than 90%, with a half-width from fractions of a degree to several degrees. The exact nature of a particular drop depends on the parameters of the coupler, the metal, and the frequency employed.

The distinction between a surface plasmon defined by total absorption and the experimentally observed structure which displays a small but nonzero reflectance may not be merely academic in the context of small but observable surface effects which we expect liquid mercury to manifest. The residual reflectance is associated with radiative damping of the surface-plasma excitation, a phenomenon which arises because light can couple out of a prism–thin-film system as well as coupling to the nonradiative mode in the first place. The existence of such a damping mechanism should cause a shift in the location of the surface resonance, this shift being engendered by the reactive effects of the outgoing radiation. The general principles governing such a shift apply to all radiatively damped resonances.[58]

We wish now to consider the influence of radiative damping on surface-plasmon dispersion, a task which is readily accomplished by evaluating the displacement of the angle of minimum reflectance as the spacer thickness d is varied. From the work of Otto on the NRSP in silver[59] it may be seen that, at a constant frequency $\omega = 3.45 \times 10^{15}$ sec^{-1}, when the spacer thickness decreases from 3000 to 1000 Å, the reflectance (in this case, actually the reflectance ratio R_{TM}/R_{TE}) increases from approximately zero to roughly 80%. The change in position of the resonance as a result of this drastic shift in radiative damping is from $\approx 54°$ incidence on the prism base to $\approx 58°$ incidence—certainly a significant change when compared with the peak separations which have been noted for the three "plausible" surface models of mercury.

The calculations presented in Fig. 12 represent the dispersion relation over several eV, a relatively large energy range. Since it proved impossible in these calculations to achieve coupling to the NRSP over the entire energy range with a single spacer thickness, d was allowed to vary with with frequency in such a way that observable surface-plasmon absorption occurred. Concomitantly, it has been necessary to take account of the influence of radiative damping on the NRSP dispersion relation. In doing so, we have tried to establish a criterion which will minimize radiative damping as a significant variable in the problem in order that differences among the dispersion relations shown in Fig. 12 may be ascribed primarily to differences in surface structure.

How can this aim be achieved? We observe at this point that the usual "incident-wave" surface plasmon is defined by a condition of constant radiative damping: To be explicit about this, the usual prescription corresponds to *no* radiative damping at any frequency, since there is no outgoing wave in the prism. By analogy with this point of view, the NRSP's which have been determined in the present investigation have also been defined on the basis of (approximately) constant radiative damping. The condition was imposed largely in an *ad hoc* way: Appropriate values of d were determined by requiring the residual reflectivity R_{TM} to remain roughly constant, at $R_{TM} \approx 0.2$, as the frequency was varied. In doing this we took advantage of the fact that the calculations described here were not limited in the same way as most experiments by the availability of prisms with only a few coating (spacer) thicknesses.

Having described the methods of computation and the numerical results of our study of NRSP excitation in liquid mercury, it is instructive to backtrack for a moment and analyze the surface-plasmon calculations in the light of Herpin's theorem,[37] in order to gain a better understanding of why the type of surface-plasmon experiment proposed here should be capable of yielding information which is basically distinct from that generated by the classical optical methods. A well-known principle in optics, Herpin's theorem states that any stratified medium—and therefore, any continuous, nonuniform medium approximated by a large number of thin homogeneous films—can be

reduced to an equivalent system composed of only two layers (equivalent meaning, e.g., that the calculated reflectances are the same). The proof of this assertion rests on the fact that each of the Herpin matrices $\underline{S}_j$ may be expressed as a linear combination of Pauli spin matrices, and therefore any continued matrix product of the $\underline{S}_j$ can also be so expressed. By appropriate choices of optical constants and thicknesses of the equivalent double layer, the continued product may thus be represented as

$$\underline{Q}=\prod_{j=1}^{N}\underline{S}_j=\underline{S}_A\cdot\underline{S}_B\ . \tag{4.5}$$

In considering the implications of Herpin's theorem for a diffuse transition layer at a liquid-metal surface, one is struck immediately by the fact that a particular double layer may be associated with several very different transition zones. Indeed, the investigations of Bloch and Rice revealed a number of models for the diffuse mercury surface, all based upon the Epstein profile (2.2), but with different values for the parameters of the quasi-free-electron and localized-state surface regions. Each profile gave rise to apparent optical constants in agreement with ellipsometric experiments, performed at about 80° incidence, and, in addition, yielded reflectances which coincided with the Drude-like measurements of Schultz,[23] at 45°, and of Bloch and Rice, near normal incidence.

From a naive point of view, the equivalence of several profiles to a single double-layer system might be taken as evidence that optical methods, surface-plasmon absorption included, are fundamentally limited in the scope of information they can reveal about an inhomogeneous surface layer. It might be further supposed, according to this line of reasoning, that all optical experiments will exhibit the same sensitivity to the structure of an inhomogeneous region, since they all appear to sample the same equivalent double layer, and should therefore produce results which are basically equivalent rather than complementary. While we accept the former argument that the relation between transition zones and a set of optical results is homeomorphic rather than isomorphic, we reject the latter assertions. To support this conclusion, and to show why optical excitation of plasma waves at a liquid-metal surface should provide a new and reasonably sensitive probe of surface structure, it is useful to reexamine Herpin's theorem somewhat more carefully.

It is to be noted, first of all, that each of the elements of the Herpin matrix $\underline{S}_j$ is a function of several variables: the parameters characterizing the jth layer, ϵ_j and δ_j, and, in addition, the frequency ω, angle of incidence θ in the homogeneous contact medium, and the dielectric constant of that medium, ϵ_d. As a result, each element of the product matrix $\underline{Q}$ incorporates a rather complicated dependence on these parameters, which in turn is exhibited in the discrepancies that occur among apparent optical constants calculated from normal-incidence and ellipsometric measurements.

Let us now assume the existence of several diffuse profiles, each fitting the apparent optical constants at a metal-dielectric interface over a wide range of angles and frequencies. We are interested in the behavior of the Herpin matrices and the equivalent double layer for a surface-plasmon experiment under conditions of frustrated total reflection. Light that is incident on the prism-film surface in such an experiment gives rise to a characteristic exponential decay of the field amplitudes in the coupling film. As is well known, this sort of field modulation corresponds to a complex angle of transmission within the spacer layer, so that the radiation is incident on the thin-film–mercury interface at a complex angle, too. It is this complex angle of incidence which distinguishes surface-plasma excitation by frustrated total reflection from other optical techniques, and which leads to its greater sensitivity to surface structure. In physical terms, the complex angle of incidence at the mercury surface results in a larger parallel momentum transfer than is possible by classical optical methods. Consequently, the decay length for the fields, given by $(\mathrm{Re}\kappa_m)^{-1}$ in a homogeneous metal, is smaller, and the surface plasmon excitation should reflect surface anomalies more strongly.

V. CONCLUSIONS AND SPECULATIVE REMARKS

The primary objective of the present section is to evaluate the results which have been obtained in Sec. IV regarding the use of NRSP spectroscopy in the study of liquid-metal surfaces, and, more generally, in the investigation of any conducting surface with nonuniform electronic structure. In performing this evaluation we analyze both the strengths and the limitations which the present work has revealed, and we suggest ways in which the sensitivity of NRSP absorption might be increased beyond that of the simple FTR technique. In the course of the discussion we also describe some simple models which have proved useful in studying the propagation of surface plasmons at imperfect surfaces; the dispersion predicted by these models for the NRSP is compared with the corresponding behavior that would be observed at a mercury surface with an Epstein transition layer. A number of important conclusions emerge from these comparisons which should contribute to our

interpretation of surface-plasmon absorption at the liquid-metal surface. In particular, we establish several criteria concerning the appearance of distinctive structure in the NRSP dispersion relation—structure which is associated with "anomalous" electronic properties at the surface.

As a beginning, let us place the present investigation in a proper perspective with respect to other studies of surface plasmons at imperfect surfaces. While most attention has been focused on their excitation at rough metal surfaces, some investigators have attempted to include electronic relaxation at a surface in a theory of surface-plasma waves. Bennett[48] has proposed a hydrodynamic model and Feibelman[49] has pursued an approach based on the random-phase approximation; in both treatments the surface plasmon shows some sensitivity to the structure of the surface transition region. We note, however, that these investigations have concentrated on the high-energy ($E \approx \hbar\omega_{sp}$), high-momentum ($\hbar k_x \gg \hbar\omega_{sp}/c$) regime, for in this range the hydrodynamic and RPA (random-phase approximation) treatments of surface plasmons yield to solution after retardation of the electromagnetic fields is neglected or a high-frequency expansion is made for the response functions of the electron gas. These models are consequently more appropriate for the description of electron-energy-loss experiments than the interpretation of "optical" surface plasmons excited by FTR. As yet, there has been no satisfactory treatment of the nature of surface-plasma waves in the low-energy region at a metal surface with an electronic transition zone. It has traditionally been assumed that the surface plasmon at these energies should be insensitive to the details of surface structure, because the mode is primarily photonlike, its dispersion curve asymptotic to the light line of the contact medium as $\omega \to 0$. But for the case of liquid mercury we have found that there is an intermediate energy range, between $E \ll \hbar\omega_{sp}$ and $E \approx \hbar\omega_{sp}$, within which the NRSP dispersion is sensitive to nonuniformities in the charge distribution. To our knowledge, the calculations of Sec. IV represent the first time that retardation effects have been systematically included in the study of surface-plasma waves in a nonuniform transition zone.

One of the limitations on NRSP spectroscopy in liquid mercury is the fact that the differences which have been calculated in optical response between an Epstein stratified mercury surface and a zero-thickness Drude or ellipsometric Fresnel surface range from only a few tenths of a degree to about 1°—not as large as might have been expected, in view of the 10% discrepancy between the apparent optical constants measured by ellipsometry and reflectance. Nonetheless, one should be able to detect these differences experimentally, particularly at higher energies where the reflectance drops are separated by several tenths of a degree or more. Distinction between these models using other criteria may be required (see Sec. VI). We note with special interest the fact that reflectance calculations for the two Bloch-Rice profiles mentioned in Sec. II, one symmetric and the other skewed, indicate that the two profiles should be distinguishable in a surface-plasmon experiment at high energies, although they correspond very nearly to the same equivalent double-layer system at lower energies and for the conventional optical techniques.

A second limitation is posed by the high degree of internal damping that exists in mercury, a phenomenon which is mathematically represented by the large imaginary part of the dielectric constant. With increasing energy this internal damping results in broadening of the resonance to a point where definition of the mode becomes problematical. As a result, it would appear difficult to observe surface plasmons in mercury by the FTR technique above 5 or 6 eV.

By imposing an external electric field at the mercury surface one might be able to overcome the limitations mentioned above and distinguish more readily the surface-plasmon absorption due to different surface models. One would expect the surface dipole layer in mercury to be enhanced by such a technique; indeed, a recent microscopic treatment of metal surfaces by Lang and Kohn[60] shows that a static external field should have precisely this effect of drawing the centers of positive and negative charge apart. An additional means of increasing the sensitivity of a surface-plasmon experiment might be to impose a modulating electric field which is slowly varying in time in conjunction with a static external field. The resulting experimental configuration would be much like the electroreflectance technique which has been widely applied to semiconductors in recent years.[61]

In addition to the measurably large shift of the NRSP dispersion in mercury towards the radiative regime, caused by the fact that the effective electron density at the Epstein stratified surface is greater than in the bulk metal, there are a number of additional features which, on theoretical grounds, might be expected to play a role in the spectrum of surface-plasma oscillations at a diffuse mercury surface. Among these features we note the possibility of interaction between the localized electronic states subsumed in- (2.6) and the collective surface-plasma mode. Just as the NRSP is known to interact with phonon modes which are localized at a surface,[11] one might anticipate a mixing of plasmon and localized electronic states. Such an interaction, if not occurring naturally between the

NRSP and the localized states arising from the metal-to-nonmetal transition in the low-density region of the surface zone, might always be introduced by alloying or by adsorption of suitable species at the mercury surface.

In an attempt to understand the NRSP–localized-state interaction, Guidotti, Rice, and Lemberg[62] have studied a simple model involving localized states which permits straightforward evaluation of the NRSP dispersion relation. The model is based on the premise that the nonuniform structure of a metal surface can be neglected, in a first approximation, when one considers interactions between the two types of electronic states. Thus, throughout the metal the dielectric function is assumed to contain a Lorentzian contribution arising from a small fraction of localized resonances in addition to the predominant contribution due to nearly-free electrons.

The dispersion relation which results from this localized-state model departs most significantly from the simple form illustrated in Fig. 2 near the localized-state resonant frequency ω_0. The curve of ω versus k_x is nearly asymptotic to the frequency ω_0 for large values of k_x, and as the energy increases it exhibits a sharp resonance-induced spike. There is a small range of energies within which the excitation appears to possess a negative group velocity. Such behavior is typical of systems in which the surface plasmon couples with other modes.

In order to evaluate the effect that localized states might have on the NRSP in mercury, several FTR calculations of the sort described in Sec. IV were performed at low energies, close to the localized-state resonance of the Epstein profile. The NRSP at these energies was found to be shifted entirely to the radiative regime, continuing the general trend for decreasing energy which is depicted in Fig. 12. While this appears to be the first time that such a drastic change has been noted for the surface-plasma excitation—from nonradiative to radiative character—there is no noticeable structure which can be ascribed to the localized states. In fact, the optical response undergoes little change even when the region of localized states is partially or completely removed from the surface transition zone, in accord with the suggested cutoff of Crozier and Murphy.[29]

Faced with an apparent discrepancy between surface-plasmon calculations in mercury and the heuristic model defined by Guidotti, Rice, and Lemberg, we take note of important differences between the two treatments. First of all, we point out that localized states in the Bloch-Rice transition zone occur over a region of only a few angstroms, a distance which is quite small when compared with the decay length for surface plasmons in mercury at optical frequencies (≈ 200 Å). By contrast, the localized resonances postulated in the simple model are assumed to occur throughout the entire metal sample. Second, in the Bloch-Rice surface layer, there is a sharp cutoff between the region of localized-state conduction and nearly-free-electron conduction. Since surface-plasma waves originate basically in oscillations of the nearly-free electrons, spatial separation of the two types of electronic states undoubtedly decreases the tendency for localized and plasmon states to interact.

In spite of the negative results which our Epstein-profile calculations indicate for surface-plasma–localized-resonance interactions, however, the localized-state model described above should be of significant value in interpreting surface diagnostic studies of liquid metals. As already mentioned, localized states may be introduced by alloying. In this connection we note that the alloy transition zones which have been fitted to experiment by Siskind, Boiani, and Rice[32] give reason to suspect that the interaction of the collective surface mode and individual electronic states may be stronger in the alloy than in a pure liquid metal. The decay length Λ associated with the differential concentration gradient in an amalgam of mercury and indium is found to be about 30 Å, a distance much larger than the region occupied by localized states in pure mercury.

There is another way in which the simple model may aid in understanding surface-plasmon absorption in mercury. The Epstein profile advanced by Bloch and Rice is based on a fit to experimental results, and as such lacks a fundamental theoretical justification. It is reasonable to suppose, therefore, that the modeled nonuniform conductivity (2.2) does not fully incorporate all features which a realistic transition zone might possess. If the Mott transition were broadened at the liquid-metal surface so that the zones of free and localized conduction processes overlap, for instance—a phenomenon which might be brought about by the mobility of the liquid-metal ions—the NRSP–localized-state mixing might well be manifested more prominently in the surface-plasmon dispersion relation.

A second model of the diffuse metal surface suggested by Guidotti, Rice, and Lemberg takes account of inhomogeneity in the charge distribution, but not of localized resonances.[62] The nonuniformity is expressed in terms of an exponential profile for the electronic density,

$$n(z) = n_b + (n_s - n_b)\, e^{-z/a} , \qquad (5.1)$$

and the assumption is made that all electrons can be treated as quasifree particles. In calculations with this exponential model, an additional nonra-

diative branch has been found in the surface-plasmon dispersion relation. This branch is located in a narrow frequency band between the surface-plasma frequency and the plasma frequency. The new branch appears to result from the fact that an inhomogeneous structure with a large gradient in its electronic properties mimics, to some extent, a system composed of a homogeneous metal substrate overlaid by a thin metal film, which is in turn bounded by a semi-infinite dielectric. In an idealized system such as this, with two metal boundaries, two surface-plasmon branches should occur, corresponding to charge oscillations which are localized at either the substrate-film or film-dielectric interfaces.

If the monotonic approximation (5.1) for the electron density at a metal surface leads to an additional branch in the spectrum of surface-plasma oscillations, it may be expected, *a fortiori*, that the Epstein profile postulated by Bloch and Rice should give rise to a second branch also. We anticipate this because the sharply peaked Epstein profile resembles a discrete film-substrate system much more closely than the exponential form (5.1). In the exponential calculations a second branch has been observed for relative surface excesses $|n_s - n_b|/n_b$ as low as 10%; by comparison, the symmetric Epstein profile with $\sigma_{0s} = 48\sigma_{0b}$ corresponds to an excess surface concentration many times larger. Moreover, the gradient of the electronic properties (e.g., conductivity) is much greater for the Epstein profile than it is for the exponential model.

Despite these favorable prospects for the appearance of a second surface-plasmon branch in mercury, a number of additional factors must be considered when we attempt to project the behavior of a real physical system such as mercury from a simple model like the one defined by (5.1). Since the work of Ehrenreich and Philipp on the optical properties of silver,[5] it has been known that the effect of interband transitions on the plasma oscillations of a conducting medium is to renormalize the plasma frequency from a quasi-free-electron value given by

$$\omega_p^0 = (4\pi ne^2/m_e)^{1/2} \tag{5.2}$$

to a value defined by the condition that the real part of the dielectric constant vanish:

$$\mathrm{Re}[\epsilon_m(\omega_p)] = 0 \ . \tag{5.3}$$

In a similar way, it should be apparent from (3.12) that the change in dielectric screening resulting from interband absorption renormalizes the surface-plasma frequency so that it satisfies

$$\mathrm{Re}[\epsilon_m(\omega_{sp})] + \epsilon_d = 0 \tag{5.4}$$

when the conductor is bounded by a medium of dielectric constant ϵ_d.

If we apply condition (5.3) and (5.4) to liquid mercury bounded by vacuum, we find from the near-normal reflection measurements of Wilson and Rice[56] that the plasma energy $E_p = \hbar\omega_p$ is renormalized from a quasifree value of 15 eV to about 7 eV for the electron gas with interactions screened by interband effects. Analogously, the surface-plasma energy $E_{sp} = \hbar\omega_{sp}$ is shifted from 10.5 eV to a screened value of 6 eV. The two energies are shifted to within about 1 eV of one another, similar to the change that is observed in silver.[5]

The importance of taking interband transitions into account becomes apparent when we consider the second NRSP branch in the light of Feibelman's microscopic analysis of interfacial plasmons at bimetallic junctions.[63] The surface-plasma frequency characterizing the bimetallic interface is given by

$$\omega_{sp}^2 = \tfrac{1}{2}(\omega_{p1}^2 + \omega_{p2}^2) \ , \tag{5.5}$$

where ω_{p1} and ω_{p2} are the plasma frequencies of the two semi-infinite metals. Feibelman points out that for $\omega_{p1} > \omega_{p2}$, the surface-plasma oscillations localized at the boundary in metal 1 will be degenerate in energy with bulk plasmons in metal 2. Therefore, surface plasmons occurring in the frequency range between ω_{p1} and ω_{p2} should be able to decay by continuous transfer of energy to the bulk modes which propagate on the low-electron-density side of the junction. Furthermore, Feibelman demonstrates that when the electron densities are in the relation $n_1 \gtrsim 3n_2$, Landau damping of the bulk mode in metal 2 becomes a significant factor, the bulk plasma oscillations then decaying into single-particle excitations of the low-density electron gas. This additional damping mechanism should be reflected in the "real" dispersion and the width of surface-plasmon absorption at the bimetallic interface.

If we turn once again to the nature of surface-plasmon propagation in mercury in the presence of a surface transition layer, we can now apply Feibelman's analysis of the surface mode at a diffuse bimetallic junction to the second branch which has been found at an inhomogeneous conducting surface that is bounded by a dielectric. As pointed out earlier in the present section, such a surface mimics the behavior of a metal-film–metal-substrate system. For the particular case of mercury, a film-substrate combination may be numerically determined[64] which possesses apparent optical constants in good agreement with ellipsometric and reflectometric measurements. The effective dc conductivity σ_{0f} of the film in this equivalent system is many times larger than the dc

conductivity of bulk mercury σ_{0b}. Equation (2.4) implies, then, that the effective density of free electrons in the film is much larger than in the bulk. Because of the latter relation, Feibelman's treatment suggests that the upper surface-plasmon branch in mercury, which corresponds to charge oscillations at the bimetallic film-substrate boundary, should be strongly damped by decay into bulk plasmons in the substrate which subsequently are strongly Landau damped.

The renormalization of plasma energies which occurs because of interband transitions, however, may alter this conclusion significantly. If interband effects in the surface layer—which undoubtedly are different from those in the bulk—lower the film plasma frequency sufficiently, the degree of Landau damping will be altered, and its influence perhaps largely eliminated. The appearance of a distinct second branch in the surface-plasmon spectrum of mercury may thus serve as a measure of the electronic interactions occurring in the surface transition zone.

The analyses presented above are, of course, highly speculative. They have not been aimed at achieving a conclusive and fully rigorous theory of surface-plasma waves in liquid mercury, as the exact nature of the surface transition zone is still largely unknown. Rather, it has been our purpose in this section to suggest several lines of profitable inquiry and to develop a conceptual structure within which a rigorous theory may eventually be defined. We believe that the present investigation marks surface-plasmon absorption by frustrated total reflection as a useful technique for the study of conducting surfaces. In conjunction with appropriate modulation, alloying, or adsorption techniques to emphasize various features of the surface, the study of surface-plasma waves should provide much information in the future on the microscopic structure of liquid-metal surfaces, as well as other interfaces characterized by nonuniformities in electronic structure.

VI. PRELIMINARY EXPERIMENTAL STUDIES

When this paper was reviewed the referee requested that it be expanded to include a comparison of theory and experiment. Since an experimental study of surface plasmons in liquid metals is underway in our laboratory we are able to include the following preliminary report of a test of the theory presented in Sec. IV. Full details of the experimental studies will be published later.

We have constructed a surface-plasmon spectrometer employing the FTR principle. Incident light is passed through a 0.3-m McPherson 218 monochromator (in the results reported below we used a 10-Å bandpass), polarized, reflected from the FTR assembly, analyzed, and detected. The

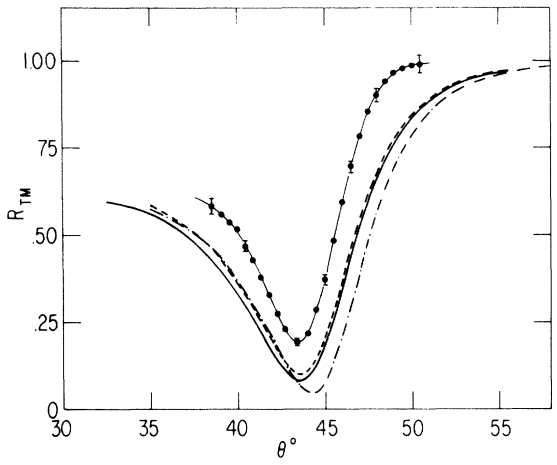

FIG. 13. Surface-plasmon line shape for liquid mercury. Points, experimental results; dashed line, ellipsometric Fresnel model using the optical constants of Faber and Smith and of Hodgson; solid line, the Bloch-Rice model; dot-dash line, Drude-Fresnel model with $\sigma_0 = 9.35 \times 10^{15}$ sec^{-1} and $\tau = 4.54321 \times 10^{-16}$ sec.

FTR assembly is mounted on a precision goniometer which is accurate to 1 second of arc. The FTR assembly consists of a stainless-steel cell which is filled by distillation (following evacuation and pumpdown to 10^{-7} Torr), closed by an IRG-2 glass prism with NaF undercoating. Various thicknesses of NaF undercoating were used, depending on the wavelength range investigated.

We display, in Figs. 13 and 14, the results of experiments on liquid Hg at room temperature. Our data indicate, unambiguously, the shortcomings of the zero-thickness Drude surface model. In Fig. 13 we compare the experimental results with the predictions of the Drude-Fresnel, the ellipsometric-Fresnel, and the Bloch-Rice surface models. As can be seen from the figure, the latter two models predict resonance minima in quite good agreement with experiment, although the observed line shape is rather narrower than that predicted. The Drude-Fresnel model, on the other hand, not only leads to a broader resonance, but, more significantly, it predicts a resonance minimum which is removed from the measured value by about 0.8°. The other two models yield minima within 0.2° of the experimental value.

At higher energies the trend is for the experimental minimum to fall between that predicted by the Bloch-Rice model and that by the ellipsometric-Fresnel model. The observed linewidths remain smaller than those predicted by these models, but the qualitative characteristics of the shape remain similar. In contrast, the Drude-Fresnel model line-shape loses even its qualitative resemblance to the experimental results, becoming very shal-

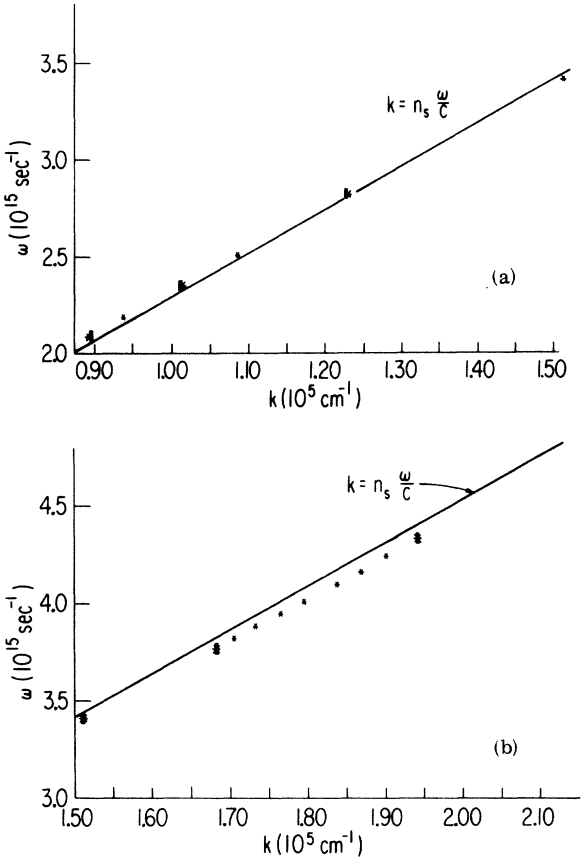

FIG. 14. (a) and (b) are the surface-plasmon dispersion curves for liquid mercury between 1 and 3 eV. The vertical lines on top of the experimental points indicate the predictions of the Bloch-Rice model.

low and broad. The resonance minimum here predicted is also in disagreement with experiment.

Although the resonance locations and resonance shapes are very similar for the Bloch-Rice and ellipsometric-Fresnel models, there is a means of distinguishing between them. As pointed out by Bloch and Rice, the ellipsometric-Fresnel model derived from a fit to ellipsometric data does not fit the reflectance data. This is apparent in Fig. 13, where there is seen to be a predicted difference in reflectance for $\theta < \theta_c$. The data available support the Bloch-Rice model.

Figure 14 shows the dispersion of surface plasmons on liquid mercury between 1 and 3 eV. Note the agreement with the predictions of the Bloch-Rice model. It should be emphasized at this point that this dispersion curve, as well as all such curves obtained in FTR measurements, do not represent a true normal-mode response of the system. Instead, they correspond to the characteristic behavior of a response function, in this case the reflectance. Attempting to associate the minima of the reflectance directly with the normal modes of the surface-plasma waves can be very misleading. One must remember that both the intrinsic damping in the system, as well as the radiative damping, contribute to a shift in the position of the minimum from that of the normal mode to that observed through the response function. Thus it is not surprising to see the dispersion curve continuously cross over the light line in Fig. 14. Both the Bloch-Rice model and the ellipsometric-Fresnel model predict this crossover, whereas the normal-mode dispersion curve based on the ellipsometric optical constants does not ever cross over the light line (this would be unphysical).

ACKNOWLEDGMENTS

Howard Lemberg wishes to thank the National Science Foundation for a predoctoral traineeship. This research has been supported by a grant from the National Science Foundation. We have also benefitted from the use of facilities provided under the Materials Laboratory Program of the National Science Foundation. We wish to thank Dr. Aaron N. Bloch for helpful conversations and stimulating criticisms provided during the execution of this work.

APPENDIX: METHODOLOGY OF NUMERICAL INTEGRATION

The numerical methods which have been employed in evaluating reflectivities from a nonuniform mercury surface are based on the treatment of the electrodynamics of stratified media set forth by Herpin.[37] In the procedure described in this appendix, it has been assumed that liquid mercury occupies the region $z \geq 0$ and is bounded by a dielectric in the half-space $z < 0$. The inhomogeneous surface layer is sliced into N thin films at positions $z = z_1, z_2, \ldots, z_N, z_{N+1}$, with successive values of z related to $z_{j+1} = z_j + \delta_j$. When the increments δ_j are small enough, we may appeal to the limiting process of the fundamental theorem of the calculus, and treat each film as though it were perfectly homogeneous. For transverse-magnetic (p-polarized) waves, therefore, the electromagnetic fields will be determined by

$$H''_{yj} = \kappa_j^2 H_{yj} \tag{A1}$$

and

$$E_{xy} = \frac{c}{i\omega\epsilon_j} H'_{yj} \tag{A2}$$

in film j, where $\kappa_j^2 = k_x^2 - (\omega^2\epsilon_j/c^2)$ and $\epsilon_j = \epsilon(z_j)$.

The most general solutions of (A1) and (A2) are readily seen to be

$$H_{yj} = c_0 e^{-\kappa_j z} + d_0 e^{\kappa_j z} \tag{A3}$$

and

$$E_{xj} = g_j (c_0 e^{-\kappa_j z} - d_0 e^{\kappa_j z}) , \tag{A4}$$

with $g_j = -c\kappa_j / i\omega\epsilon_j$. However, instead of working with the fields directly, the Herpin method is expressed in terms of auxiliary quantities X_j and Y_j which are given by

$$\begin{aligned} X_j &= -g_j H_{yj} + E_{xj} = -2g_j d_0 e^{\kappa_j z} , \\ Y_j &= -g_j H_{yj} - E_{xj} = -2g_j c_0 e^{-\kappa_j z} . \end{aligned} \tag{A5}$$

Matrices $\underline{A}$ and $\underline{Z}$ are now defined by

$$\underline{A} = \begin{pmatrix} H_y \\ E_x \end{pmatrix} , \tag{A6}$$

$$\underline{Z} = \begin{pmatrix} Y \\ X \end{pmatrix} \tag{A7}$$

and are specified at a discrete set of points by appropriate labeling. We set

$$\begin{aligned} \underline{A}_j &= \underline{A}(z_{j+1}^-) , \\ \underline{A}_j' &= \underline{A}(z_j^+) \end{aligned} \tag{A8}$$

and

$$\begin{aligned} \underline{Z}_j &= \underline{Z}(z_{j+1}^-) , \\ \underline{Z}' &= \underline{Z}(z_j^+) , \end{aligned} \tag{A9}$$

and note that by labeling in this manner, all matrices with subscript j are defined at points in film j.

From the definitions (A8) and (A9), it may now be shown that the primed and unprimed are related by

$$\underline{Z}_j' = \underline{P}_j \underline{Z}_j , \tag{A10}$$

where

$$\underline{P}_j = \begin{pmatrix} e^{\kappa_j \delta_j} & 0 \\ 0 & e^{-\kappa_j \delta_j} \end{pmatrix} \tag{A11}$$

and also by

$$\begin{aligned} \underline{Z}_j' &= \underline{T}_j \underline{A}_j' , \\ \underline{Z}_j &= \underline{T}_j \underline{A}_j , \end{aligned} \tag{A12}$$

with

$$\underline{T}_j = \begin{pmatrix} -g_j & -1 \\ -g_j & 1 \end{pmatrix} . \tag{A13}$$

In addition, the tangential electric and magnetic fields must be continuous at all the film boundaries, so that

$$\underline{A}_j' = \underline{A}_{j-1} \tag{A14}$$

must hold for all values of j. By combining (A10)–(A14), it follows that

$$\underline{Z}_{j-1} = \underline{T}_{j-1} \underline{A}_{j-1} = \underline{T}_{j-1} \underline{A}_j' = \underline{T}_{j-1} \underline{T}_j^{-1} \underline{Z}_j' = \underline{T}_{j-1} \underline{T}_j^{-1} \underline{P}_j \underline{Z}_j . \tag{A15}$$

Consequently, from (A12), it may be seen that

$$\underline{A}_{j-1} = \underline{T}_j^{-1} \underline{P}_j \underline{T}_j \underline{A}_j = \underline{S}_j \underline{A}_j , \tag{A16}$$

where the matrix

$$\underline{S}_j = \underline{T}_j^{-1} \underline{P}_j \underline{T}_j \tag{A17}$$

performs the necessary translations and rotations in relating the matrix $\underline{A}$ in the $(j-1)$st film to its value in the jth film. But (A16) implies that

$$\underline{A}_0 = \underline{S}_1 \underline{A}_1 = \underline{S}_1 \underline{S}_2 \underline{A}_2 = \underline{S}_1 \underline{S}_2 \cdots \underline{S}_N \underline{A}_N = \underline{Q}_N \underline{A}_N , \tag{A18}$$

where

$$\underline{Q} = \prod_{j=1}^{N} \underline{S}_j , \tag{A19}$$

providing us with a relation between the incident and reflected fields in the bounding dielectric and the transmitted field in bulk mercury. We note that

$$\underline{A}_0 = \begin{pmatrix} H_y \\ E_x \end{pmatrix}_{\text{at } z_1^-} = \begin{pmatrix} H_{yi} + H_{yr} \\ E_{xi} + E_{xr} \end{pmatrix} \tag{A20}$$

and

$$\underline{A}_N = \underline{A}_{N+1}' = \begin{pmatrix} H_y \\ E_x \end{pmatrix}_{\text{at } z_{N+1}^+} = \begin{pmatrix} H_{yt} \\ E_{xt} \end{pmatrix} . \tag{A21}$$

In the present geometry the incident, reflected, and transmitted magnetic fields are given by

$$\begin{aligned} H_{yi} &= d_0 e^{\kappa_0 z} , \\ H_{yr} &= c_0 e^{-\kappa_0 z} , \\ H_{yt} &= b_0 e^{-\kappa_b z} , \end{aligned} \tag{A22}$$

so, by (A2), the corresponding tangential electric fields are just

$$\begin{aligned} E_{xi} &= -g_0 H_{yi} , \\ E_{xr} &= -g_0 H_{yr} , \\ E_{xt} &= g_b H_{yt} . \end{aligned} \tag{A23}$$

From (A18)–(A23) we then have

$$\begin{aligned} H_{yi} + H_{yr} &= (Q_{11} + g_b Q_{12}) H_{yt} , \\ -g_0 (H_{yi} - H_{yr}) &= (Q_{21} + g_b Q_{22}) H_{yt} , \end{aligned} \tag{A24}$$

from which the amplitude reflection coefficient for p-polarized radiation may be found:

$$r_p = \frac{H_{yr}}{H_{yi}} = \frac{g_0 (Q_{11} + g_b Q_{12}) + (Q_{21} + g_b Q_{22})}{g_0 (Q_{11} + g_b Q_{12}) - (Q_{21} + g_b Q_{22})} . \tag{A25}$$

For transverse-electric (s-polarized) waves, the field equations in film j are

$$E''_{yj} = \kappa_j^2 E_{yj} , \tag{A26}$$

$$H_{xj} = -(c/i\omega) E'_{yj} , \tag{A27}$$

which have the general solutions

$$E_{yj} = c_0 e^{-\kappa_j z} + d_0 e^{\kappa_j z} , \tag{A28}$$

$$H_{xj} = -\epsilon_j g_j (c_0 e^{-\kappa_j z} - d_0 e^{\kappa_j z}) . \tag{A29}$$

Comparing the form of (A28) and (A29) with expressions (A3) and (A4), we recognize that the Herpin analysis for s-polarized radiation must be equivalent to the formal development for p-polarized light, when the following substitutions are made:

$$H_y \rightarrow E_y ,$$

$$E_x \rightarrow H_x ,$$

$$g_j \rightarrow -\epsilon_j g_j . \tag{A30}$$

Thus, from (A25), the reflection coefficient for s-polarized waves is just

$$r_s = \frac{E_{yr}}{E_{yi}} = \frac{\epsilon_0 g_0 (Q_{11} - \epsilon_b g_b Q_{12}) - (Q_{21} - \epsilon_b g_b Q_{22})}{\epsilon_0 g_0 (Q_{11} - \epsilon_b g_b Q_{12}) + (Q_{21} - \epsilon_b g_b Q_{22})} , \tag{A31}$$

assuming the substitutions (A30) have been made in defining the matrix also. Finally, the reflectivities R_p and R_s are determined by the square of the absolute value of the reflection coefficients:

$$R_p = r_p r_p^* = |r_p|^2 ,$$

$$R_s = r_s r_s^* = |r_s|^2 . \tag{A32}$$

Equations (A25) and (A31) yield the reflection coefficients r_p and r_s for a diffuse mercury surface in contact with a single dielectric medium. The calculations presented in Sec. IV, however, refer to the FTR geometry indicated in Fig. 3, where a thin dielectric spacing film s has been inserted between the prism p and the liquid metal in order to make coupling to the NRSP possible. The reflectivity R_{TM} quoted is the internal reflectivity within the prism.

Since the spacing layer is a homogeneous film, it may be formally treated, within the scope of Herpin's method, as an additional film characterized by dielectric constant ϵ_s and thickness δ_s. Thus, the spacer has its own Herpin matrix $\underline{S}_s$ determined by (A17), and an effective matrix $\underline{Q}^{FTR}$ can be defined which incorporates the presence of the spacing film as well as the nonuniform transition zone of mercury:

$$\underline{Q}^{FTR} = \underline{S}_s \underline{Q} , \tag{A33}$$

where $\underline{Q}$ is given by (A19). Using $\underline{Q}^{FTR}$ in place of $\underline{Q}$ in Eqs. (A25) and (A31), reflection coefficients within the prism are specified, the prism p now playing the role of medium 0.

---

*Abstracted in part from the Ph.D. thesis of Howard L. Lemberg, Dept. of Chemistry, University of Chicago, 1973.

[1]D. Bohm and D. Pines, Phys. Rev. 92, 609 (1953).

[2]J. M. Ziman, *Principles of the Theory of Solids* (Cambridge U. P., Cambridge, England, 1964), pp. 237 ff.

[3]See, e.g., F. Stern, in *Solid State Physics*, edited by F. Seitz and D. Turnbull (Academic Press, New York, 1963), Vol. XV, pp. 370 ff.

[4]A. Mooradian, Phys. Rev. Lett. 20, 1102 (1968); D. C. Hamilton and A. L. McWhorter, in *Proceedings of the International Conference on Light Scattering Spectra of Solids*, edited by G. B. Wright (Springer-Verlag, New York, 1969), p. 309.

[5]H. Ehrenreich and H. R. Philipp, Phys. Rev. 128, 1622 (1962).

[6]A. Mooradian and G. B. Wright, Phys. Rev. Lett. 16, 999 (1966).

[7]See, e.g., P. M. Platzman and P. A. Wolff, *Waves and Interactions in Solid State Plasmas* (Academic Press, New York, 1973), pp. 90 ff.

[8]R. H. Ritchie, Phys. Rev. 106, 874 (1957).

[9]K. L. Kliewer and R. Fuchs, Phys. Rev. 153, 498 (1967); E. N. Economou, Phys. Rev. 182, 539 (1969).

[10]J. M. Elson and R. H. Ritchie, Surf. Sci. 30, 178 (1972).

[11]R. J. Wallis and J. J. Brion, Solid State Commun. 9, 2099 (1971).

[12]J. G. Endriz and W. E. Spicer, Phys. Rev. 184, 4144 (1971).

[13]J. L. Stanford, J. Opt. Soc. Am. 60, 49 (1970).

[14]H. Raether, in *The Structure and Chemistry of Solid Surfaces*, edited by G. A. Somorjai (Wiley, New York, 1969), p. 10-1.

[15]For a recent theoretical treatment of this topic, see D. M. Newns, Phys. Rev. B 1, 3304 (1970).

[16]J. Bardeen, Phys. Rev. 49, 653 (1936).

[17]F. Forstmann and J. B. Pendry, Z. Phys. 235, 75 (1970).

[18]A. N. Bloch and S. A. Rice, Phys. Rev. 185, 933 (1969).

[19]N. D. Lang and W. Kohn, Phys. Rev. B 1, 4555 (1970).

[20]C. A. Broxton and R. P. Ferrier, J. Phys. C 4, 1909 (1971); C. A. Croxton, Adv. Phys. 22, 385 (1973).

[21]J. E. Faber and N. V. Smith, J. Opt. Soc. Am. 58, 102 (1968).

[22]J. N. Hodgson, Philos. Mag. 4, 189 (1959).

[23]L. G. Schultz, J. Opt. Soc. Am. 47, 64 (1957).

[24]R. H. Ritchie and R. E. Wilems, Phys. Rev. 178, 372 (1969); J. M. Elson and R. H. Ritchie, Phys. Rev. B 4, 4129 (1971).

[25]H. L. Lemberg, S. A. Rice, P. H. Naylor, and A. N. Bloch, Solid State Commun. 14, 1097 (1974).

[26]P. Drude, *Theory of Optics*, translated by C. R. Mann and R. A. Milliken (University of Chicago Press, Chicago, 1902).

[27]P. S. Epstein, Proc. Natl. Acad. Sci. USA 16, 627 (1930); C. A. Eckart, Phys. Rev. 35, 1303 (1930).

[28]N. F. Mott, Proc. Phys. Soc. Lond. A 62, 416 (1949).

[29]E. D. Crozier and E. Murphy, Can. J. Phys. 50, 1914 (1972).

[30]N. R. Comins, Philos. Mag. 25, 817 (1972).
[31]W. J. Choyke, S. H. Vosko, and T. W. O'Keeffe, Solid State Commun. 9, 361 (1971).
[32]B. Siskind, J. Boiani, and S. A. Rice, Can. J. Phys. 51, 894 (1973).
[33]This well-known phenomenon follows from an elementary thermodynamic analysis. See, e.g., G. N. Lewis and M. Randall, *Thermodynamics* (revised), edited by K. S. Pitzer and L. Brewer (McGraw-Hill, New York, 1961).
[34]F. Stern, in *Solid State Physics*, edited by F. Seitz and D. Turnbull (Academic, New York, 1963), Vol. XV, p. 299.
[35]J. A. Stratton, *Electromagnetic Theory* (McGraw-Hill, New York, 1941), pp. 492 ff. It has recently been suggested e.g., by F. Sauter, Z. Phys. 203, 488 (1967), that the classical Fresnel equations comprise an incomplete description of metal optics. We shall neglect the proposed breakdown, though, as the present work deals exclusively with frequencies less than the plasma frequency.
[36]A. Ravi, D. A. King, and N. Sheppard, Trans. Faraday Soc. 64, 3358 (1968).
[37]A. Herpin, C. R. Acad. Sci. (Paris) 225, 182 (1947). The implications of Herpin's theorem for the liquid-metal surface have been considered at length in Ref. 18, and are discussed further in Sec. IV of this paper.
[38]C. W. Tucker, Jr. and C. B. Duke, Surf. Sci. 29, 237 (1972).
[39]P. J. Estrup and E. G. McRae, Surf. Sci. 25, 1 (1971).
[40]Particular difficulties are involved in interpreting LEED data at liquid, as opposed to solid, metal surfaces because of the lack of translational order. These have been discussed by G. A. Somorjai and H. H. Farrell, in *Advances in Chemical Physics*, edited by I. Prigogine and S. A. Rice (Wiley-Interscience, New York, 1971), Vol. XX, p. 215.
[41]Reference 2, p. 241.
[42]A. Otto, Z. Phys. 216, 398 (1968); A. S. Barker, Jr., Phys. Rev. Lett. 28, 892 (1972).
[43]N. Marshall and B. Fischer, Phys. Rev. Lett. 28, 811 (1972).
[44]V. V. Bryksin, Yu. M. Gerbshtein, and D. N. Mirlin, Fiz. Tverd. Tela 13, 2125 (1971) (Sov. Phys.-Solid State 13, 1779 (1972)].
[45]R. Ruppin, Solid State Commun. 8, 1129 (1970).
[46]R. Fuchs and K. L. Kliewer, Phys. Rev. B 3, 2270 (1971).
[47]J. Harris and A. Griffin, Can. J. Phys. 48, 2592 (1970); Phys. Rev. B 3, 749 (1971); J. Harris, Phys. Rev. B 4, 1022 (1971).
[48]A. J. Bennett, Phys. Rev. B 1, 203 (1970).
[49]P. J. Feibelman, Phys. Rev. Lett. 30, 975 (1973).
[50]The form of Maxwell's field equations appropriate to a conducting medium is discussed in J. D. Jackson, *Classical Electrodynamics* (Wiley, New York, 1962).
[51]G. E. H. Reuter and E. H. Sondheimer, Proc. Phys. Soc. Lond. A 195, 336 (1948).
[52]Reference 2, pp. 223 ff.
[53](a) Reference 47, p. 336; (b) S. N. Jasperson and S. E. Schnatterly, Phys. Rev. 188, 759 (1969).
[54]R. J. Bell, R. W. Alexander, Jr., W. F. Parks, and G. Kovener, Opt. Commun. 8, 147 (1973).
[55]Y. Y. Teng and E. A. Stern, Phys. Rev. Lett. 19, 511 (1967).
[56]E. G. Wilson and S. A. Rice, Phys. Rev. 145, 55 (1966).
[57]S. A. Rice, D. Guidotti, H. L. Lemberg, W. C. Murphy, and A. N. Bloch, *Advances in Chemical Physics*, edited by I. Prigogine and S. A. Rice (Wiley-Interscience, New York, to be published).
[58]The Lamb shift is perhaps the best-known shift accompanying the radiative interactions of a charged particle, although in that case the change (in the effective mass of a free electron) arises from second-order, rather than first-order, perturbative terms—i.e., electron–virtual-state coupling. Similar level shifts occur in atomic systems as well. See, e.g., the classical treatment of Ref. 50, pp. 578 ff.
[59]A. Otto, Z. Phys. 219, 227 (1969).
[60]N. D. Lang and W. Kohn, Phys. Rev. B 7, 3541 (1973).
[61]M. Cardona, *Modulation Spectroscopy* (Academic, New York, 1969), pp. 165 ff.
[62]D. Guidotti, S. A. Rice, and H. L. Lemberg, Solid State Commun. 15, 113 (1974).
[63]P. J. Feibelman, Phys. Rev. B 3, 2971 (1971).
[64]H. L. Lemberg (unpublished results).